Photoisomerization and Photoionization of the Photoactive Yellow Protein Chromophore in Solution

Delmar S. Larsen,* Mikas Vengris,* Ivo H. M. van Stokkum,* Michael A. van der Horst,† Frank L. de Weerd,* Klaas J. Hellingwerf,† and Rienk van Grondelle*

*Faculty of Sciences, Vrije Universiteit Amsterdam, 1081 HV Amsterdam, The Netherlands; and †Department of Microbiology, Swammerdam Institute for Life Sciences, University of Amsterdam, 1018 WS Amsterdam, The Netherlands

ABSTRACT Dispersed pump-dump-probe spectroscopy has the ability to characterize and identify the underlying ultrafast dynamical processes in complicated chemical and biological systems. This technique builds on traditional pump-probe techniques by exploring both ground- and excited-state dynamics and characterizing the connectivity between constituent transient states. We have used the dispersed pump-dump-probe technique to investigate the ground-state dynamics and competing excited-state processes in the excitation-induced ultrafast dynamics of thiomethyl *p*-coumaric acid, a model chromophore for the photoreceptor photoactive yellow protein. Our results demonstrate the parallel formation of two relaxation pathways (with multiple transient states) that jointly lead to two different types of photochemistry: *cis-trans* isomerization and detachment of a hydrated electron. The relative transition rates and quantum yields of both pathways have been determined. We find that the relaxation of the photoexcited chromophores involves multiple, transient ground-state intermediates and the chromophore in solution does not generate persistent photoisomerized products, but instead undergoes photoionization resulting in the generation of detached electrons and radicals. These results are of great value in interpreting the more complex dynamical changes in the optical properties of the photoactive yellow protein.

INTRODUCTION

The photoactive yellow protein (PYP) is a small, 125 amino acid-containing, water-soluble protein found in the bacterium *Halorhodospira halophila* and is responsible for triggering the negative phototaxis response of the organism to blue light (Sprenger et al., 1993; Cusanovich and Meyer, 2003; Hellingwerf et al., 2003). PYP contains an intrinsic chromophore, *p*-coumaric acid, which is covalently bound to the protein backbone via a cysteine residue (Baca et al., 1994; Genick et al., 1997; Hoff et al., 1994a). Upon photoexcitation, this chromophore undergoes a *trans-cis* isomerization around its double bond (Genick et al., 1997, 1998; Perman et al., 1998) and initiates a complicated series of reversible reactions that extends over 15 decades in time extending from femtoseconds to seconds (Baltuška et al., 1997; Brudler et al., 2001; Gensch et al., 2002; Xie et al., 2001). These isomerization-induced processes include chromophore protonation (Xie et al., 1996, 2001), protein unfolding (Brudler et al., 2001), hydrogen-bond disruption (Chosrowjan et al., 1998; Zhou et al., 2001), and their corresponding recovery reactions. Hence, PYP is an excellent system for studying the complex relationship between protein dynamics and chemical reaction dynamics and more specifically how nature has tuned both to produce biological function.

A simple, yet often unanswered, question arises when investigating protein-chromophore dynamics: Is the observed dynamics dictated by the inherent dynamics of the chromophore, or is it the result of the chromophore interacting with the protein environment? Only studying the inherent dynamics of the PYP chromophore, independent of the effects from the protein environment, and the subsequent comparison with corresponding PYP data can address this question. Ultrafast pump-probe studies of PYP have shown rich and complex dynamics of multiple species that overlap both temporally and spectrally, requiring intricate modeling schemes for interpretations (Changenet-Barret et al., 2002, 2001; Larsen et al., 2003b). To better understand the underlying nature of this complicated system, we have studied the dynamics of the isolated PYP chromophore in solution with a powerful ultrafast multipulse technique.

In this article, we investigate the photoinduced dynamics of two model PYP chromophores, thiomethyl *p*-coumaric acid (TMpCA) and thio-methyl-7-hydroxycoumaric acid, which is referred to here as thiomethyl locked (TML) in aqueous solution (Fig. 1) (Larsen et al., 2003b). Several PYP chromophore model compounds have been studied earlier (Xie et al., 2001): *p*-coumaric acid (Changenet-Barret et al., 2001) and thio-phenyl-*p*-coumaric ester (or S-phenyl thio-*p*-hydroxycinnamate) (Changenet-Barret et al., 2002); however, we consider the TMpCA chromophore the best probe to explore the dynamics of the free chromophore without potential interfering signals from the protein environment. The thio-ester linkage in TMpCA is identical to the linkage of the PYP chromophore to the cysteine residue of the protein backbone, where the methyl group acts as an inert and small capping group and hinders the observed dynamics less than would be expected with larger, bulkier groups. Moreover, we find that TMpCA exhibits a higher photostability than other studied model chromophores.

Submitted October 27, 2003, and accepted for publication November 24, 2003.

Address reprint requests to Delmar S. Larsen, Fax: 31-20-444-7999; E-mail: dslarsen@nat.vu.nl.

0006-3495/04/04/2538/13 $2.00

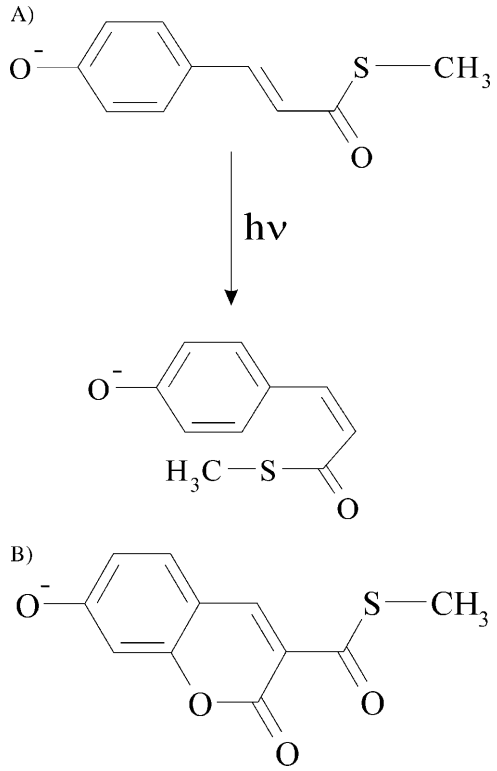

FIGURE 1 Structures of model chromophores of PYP in water at pH 10.5. (*A*) Scheme of the proposed isomerization reaction of the *trans* isomer of TMpCA into the *cis* isomer. (*B*) The TML chromophore.

Since the PYP chromophore is known to isomerize after excitation when embedded in the PYP protein environment (Kort et al., 1996; Cusanovich and Meyer, 2003; Hellingwerf et al., 2003), it is expected that the free chromophore in solution would similarly isomerize upon excitation (compare Fig. 1 *A*). To explore the role of this torsional freedom in the photoinduced dynamics, we contrasted the TMpCA results with those collected for TML, which lacks this degree of freedom, but is similar in other respects.

Pump-dump-probe (PDP) spectroscopy (also referred to as stimulated emission pumping) has successfully been used in gas phase experiments (Ishikawa et al., 1997; Pique et al., 1988) and recently has also been applied to study several biological systems in the liquid phase (Changenet-Barret et al., 2000; Gai et al., 1997; Ruhman et al., 2002; Yan et al., 2001). We have expanded these studies by measuring dispersed PDP signals (in contrast to individual wavelength traces), which allows for the simultaneous collection of both wavelength-resolved and time-resolved data (Larsen et al., 2003a). Furthermore, we use global analysis to take full advantage of these complex signals and incorporate the dump-induced changes into the underlying dynamics of the studied system (Hoff et al., 1994b). The combination of measuring dispersed PDP signals, simultaneously with pump-probe signals, and the use of global analysis to interpret both, is a powerful improvement, as contrasted to single-trace PDP measurements.

The utility of PDP spectroscopy lies in its ability to ''control'' reactions as they evolve by manipulating the population of transient species with applied laser pulses. This is, to a certain extent, related to ''coherent control'' mechanisms, where reactions are manipulated via complex processes such as vibrational wavepacket motion, quantum interferences, and electronic coherences (Rice and Zhao, 2000). A more appropriate term for describing our experiment is ''*in*coherent control'', since the data is interpreted solely in terms of manipulated electronic state populations. This simplification, as will be shown in the following analysis, allows for clear interpretations of the measured data. We identify two important aspects of the TMpCA system with the PDP technique that cannot be directly extracted from pump-probe measurements: 1), the identification of and distinction between ground-state and electronically excited intermediates and the characterization of their dynamics; and 2), the disentangling of complex reaction pathways.

MATERIALS AND METHODS

Sample preparation

The model chromophores were synthesized from *p*-coumaric acid (using the 1,1-carbonyldiimidazole derivative of the chromophore) for TMpCA and 7-hydroxycoumarin-3-carboxylic acid for TML with sodium thiomethoxide (Acros Organics, Geel, Belgium). Equimolar amounts were mixed and allowed to react overnight at room temperature. The compound was purified with a silica gel column by washing with two column volumes of petroleum ether, and elution with a 1:1 ethylacetate/petroleum ether mixture. The identity and purity of the synthesized TMpCA were confirmed with mass spectrometry and NMR analysis. The samples were buffered with 10 mM of CAPS buffer to a pH of 10.5 and were prepared with optical densities (OD) between 0.5 and 0.7 per mm. These conditions best simulate the environment found for the chromophore in the native PYP protein (Kroon et al., 1996). In both the PYP protein and in alkaline solution, the phenolic moiety of the chromophores is deprotonated, thus making it anionic (Larsen et al., 2003b).

Ultrafast spectroscopy

The important components in our experimental setup are highlighted in Fig. 2. Part of the experimental setup (the dispersed pump-probe portion) has been described before (Gradinaru et al., 2000; Larsen et al., 2003b), but is described here with some significant modifications for collecting the dispersed PDP signals. An amplified Ti:Sapphire laser system (Coherent (Santa Clara, CA) and BMI (Evry, France) Alpha 1000) operating at 1 kHz produces short duration (~60 fs full width at half-maximum) laser pulses at 790 nm with ~450 μJ/pulse. These amplified laser pulses are subsequently split into three parts. The first portion is frequency-doubled in a 0.5 mm BBO crystal, producing excitation light at 395 nm and is used as an excitation source. A second portion is used to generate a white-light continuum by focusing into a 2 mm thick, slowly translating CaF_2 plate with a 10 cm singlet lens. This continuum extends from 320 nm to the near infrared and is used as a probe beam. The remaining portion of the 790 nm pulses is used to operate a home-built, 395 nm pumped noncollinear optical parametric amplifier (NOPA) that is tuned to generate dump pulses at 505

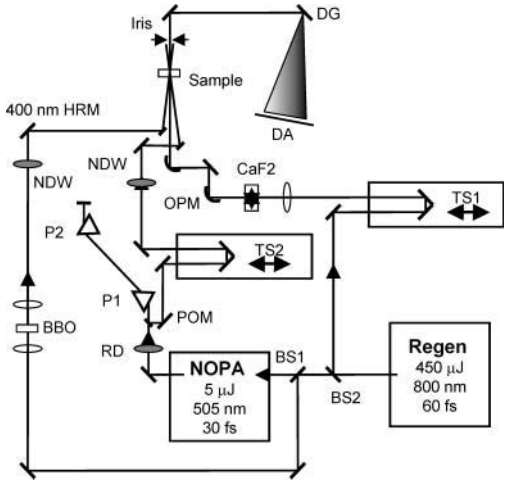

FIGURE 2 Optical layout of the pump-dump-probe experimental setup. NOPA, noncollinear optical parametric amplifier; REGEN, regenerative amplifier; POM, pick off mirror; BBO, BBO doubling crystal; NDW, neutral density wheel; HRM, high reflector mirror; P, prisms; OPM, off-axis parabolic mirrors; BS, 20% reflection beam splitter; TS, motorized translation stage; CaF2, calcium fluoride disk; DG, diffraction grating; RD, rotating disk; DA, diode array.

nm. The generated 505 nm dump pulses are then compressed with two LK7 equilateral prisms. The pulse intensities for the pump and dump pulses were ~150 nJ each.

Both the pump and the dump beams are focused in the sample (spot size ~300 μm) with separate 10 cm focal length quartz lenses, and the probe light is focused (spot size ~120 μm) with the use of off-axis (90°) parabolic mirrors to reduce dispersion. After the spatial and specified temporal overlap of all three beams in the sample, the white light probe pulse is dispersed in a spectrograph (Oriel, Stratford, CT) onto a home-built dual-diode array shot-to-shot camera. Each transient spectrum collected contains ~5000 individual spectra. Two nonphase-locked choppers were used to modulate the pump-beam (250 Hz) and the dump beam (125 Hz) independently; ~6% of the laser pulses were slightly clipped by the chopper blade and were excluded from the averaging of the data. The use of two independent choppers results in the collection of four separate signals, which can be used to generate pump-probe, pump-dump-probe, and dump-probe signals. The latter of these does not contain chromophore signals because the dump beam is nonresonant with the ground-state absorption of the TMpCA chromophore, although it does contain cross-phase modulation and scattering contributions that are used to reduce these artifacts in the other signals.

The instrument response function is 120 fs (full width at half-maximum), the wavelength resolution is 1 nm, and the polarizations of the pump and dump beam are parallel to each other, whereas the white light probe is set at magic angle (54.7°) to eliminate effects of reorientational dynamics in the sample. The dispersion of the continuum is estimated at ~300 fs over the range of 320 nm–600 nm and is accounted for in the multiwavelength global analysis. Since the pump-dump-probe technique is a multidimensional spectroscopy and requires separate and independent timing between the applied laser pulses, two computer-driven mechanical translation stages are used to vary the timing of the dump and the probe pulses. A rapidly rotating thin glass disk (<1 mm) was inserted into the pump beam line to randomize the phase relationship between the two laser beams and thus exclude coherent contributions to the collected signals. Hence, the signals presented here represent dynamics that are unaffected by the phase relationship between the laser pulses.

Traditional pump-probe techniques involve the application of two short pulses (pump and probe) onto the sample, generating one-dimensional data. When the probe is a broad-band pulse and is dispersed, an additional wavelength dimensional is introduced creating two-dimensional data. The introduction of an additional pulse between the pump and the probe pulses generates three-dimensional signals, with two time delays and one wavelength. Measuring and presenting the data in various ways exploit the multidimensionality of these signals.

The most direct way to collect such data is in the form of a ''kinetic trace'' (Fig. 3), where both the first and second laser pulses are set at fixed times and the signals are collected by varying the probe pulse delay (e.g., in pump-probe experiments). In kinetic traces, the collected data can be directly (albeit not necessarily easily) decomposed into the time-dependent spectra associated with the comprising species (vide infra).

An alternative procedure for collecting and viewing PDP signals, which is useful for identifying the connectivity between transient states in pump-probe spectra, is through recording of ''action traces''. In contrast to kinetic traces, action traces are measured by delaying the second (dump) pulse with fixed pump and probe pulses (Fig. 3). By scanning the second dump delay (with fixed probe time), the temporal efficiency of influencing the specific pump-probe (PP) spectrum is directly monitored (Larsen et al., 2003a). Hence, action traces monitor the dump-induced changes in the system response further ''upstream'' from the dumping time. By scanning over multiple dump times, the temporal dumping effect on the species observed at the given probe delay can be characterized along with the associated spectral changes.

The absorption spectrum of TMpCA and TML is shown in Fig. 4 with overlapping the spectra of the pump- and dump-laser pulses. The wavelength of the dump pulse was selected to overlap well with the stimulated emission but poorly with the ground-state absorption (GSA).

Data analysis

Whereas kinetic traces directly monitor the dump process, action traces measure their asymptotic effect at a specific probe time. In both modes, it is useful to analyze the dump-induced changes to the PP signals, resulting in double-difference signals, $\Delta\Delta$OD:

$$\Delta\Delta\mathrm{OD}(\lambda, t_{\mathrm{dump}}, t_{\mathrm{probe}}) = \mathrm{PDP} - \mathrm{PP} - \mathrm{DP}, \qquad (1)$$

where PP and DP are the pump-probe and dump-probe spectra, respectively. Since the dump-probe signals are nonresonant with both the TMpCA and TML samples, they contain only scatter from the dump pulse (~505 nm) and cross-phase modulation artifacts (across the whole probe range). However, both interfering contributions, which also exist in the pump-probe and the PDP signals, can be (mostly) removed from the $\Delta\Delta$OD signal by subtracting the artifact containing the dump-probe signal; this aids in the observation and interpretation of the fast dump-induced dynamics. The $\Delta\Delta$OD signals will contain negative excited-state (e.g., excited-state absorption and

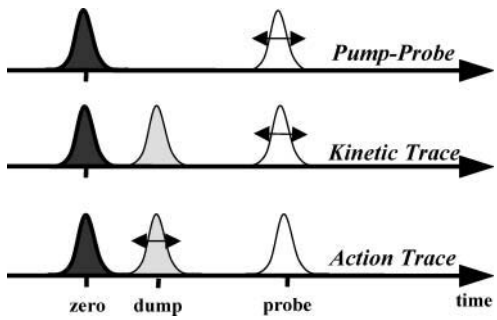

FIGURE 3 Timing schematic of the three experimental detection schemes presented here. The represented pulses are the pump pulse (*dark shaded Gaussian*), the dump pulse (*light shaded Gaussian*), and the white-light probe (*open Gaussian*).

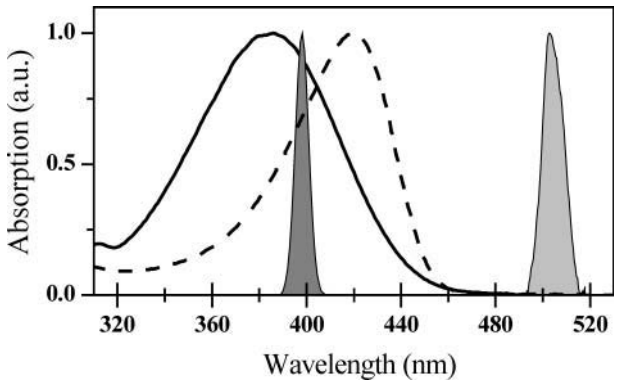

FIGURE 4 Normalized absorption spectrum of TMpCA (*solid line*) and TML (*dashed line*) at pH 10.5 and the spectra of the pump (*dark shaded filled*) and the dump (*light shaded filled*) laser pulses.

stimulated emission) signals from the depletion and positive ground-state signals, which will fill the ground-state bleach (GSB), though not necessarily instantly (vide infra). In this article, the PDP term refers to both this specific multipulse experiment and to the signals that result with both pump and dump pulses interacting with the sample (in contrast to PP or DP signals); the context dictates which definition is intended.

An important goal of applying the PDP technique to the TMpCA system is to identify and characterize the connectivity between the observed dynamical states. To elucidate such details about the system under investigation, we used a sophisticated multiwavelength global analysis approach to fit a postulated dynamical model with discrete transient states to the collected pump-probe and PDP data (Hoff et al., 1994b; Holzwarth, 1996). Central to this type of analysis is the construction of a connectivity scheme, k_{ij} that describes the interactions between the observed time-resolved states, $n_j(t)$. Assuming first-order rate kinetics, a series of differential equations is then constructed and solved that describe the time evolution of the constituent transient states:

$$\dot{n}_i(t) = \sum_j k_{ij} n_j(t). \tag{2}$$

Spectral information is introduced by adding explicit wavelength dependence to the solution obtained, resulting in the generation of wavelength-dependent factors,

$$D(\lambda, t; k_{ij}) = \sum_i A_i(\lambda) n_i(t; k_{ij}), \tag{3}$$

where $D(\lambda, t; k_{ij})$ is the noise-free absorption difference signal that can directly be compared with the experimentally collected data. The resulting wavelength-dependent factor, $A_i(\lambda)$, is the species associated difference spectrum (SADS) for the *i*th transient state. The SADS in combination with the connectivity scheme and the corresponding decay times provide an easy approach for interpreting the complex dispersed pump-probe and PDP data collected in our experiment. The SADS and timescales that relate the growth and decay kinetics associated with these individual states are estimated from the data by means of nonlinear regression. An important underlying aspect of this approach is that the measured signals can be decomposed into a set of connected states/species each with a distinguished decay time and spectrum. Although this state-to-state evolution assumption is valid for describing the dynamics of many systems, for some processes (e.g., solvation), this approach only mimics the observed dynamics. Despite this, the underlying timescales and spectral responses are still well described within the discrete modeling framework of such an analysis. The alternative global-fitting technique, most appropriate for solvation dynamics with a continuously shifting spectral band, would be to fit the multidimensional data with a continuum of transient states, all dynamically and spectrally connected. However, this is a numerically unwieldy and unstable procedure for fitting our transient absorption data and does not improve the underlying interpretation of the collected data.

RESULTS

Pump-probe signals

The ultrafast pump-probe signals for TMpCA in solution have previously been published (Larsen et al., 2003b) and exhibit complex dynamics. Some discussion of the pump-probe signals is required for understanding the information that the PDP technique provides when applied to the TMpCA system. Plotted in Fig. 5 are five dispersion-corrected pump-probe transient spectra, each exhibiting several spectral bands. The early time spectra exhibit the following four distinct bands: i), a stimulated emission (SE) band peaking at 500 nm (after relaxation), ii), a positive band at 440 nm, iii), a GSB at 380 nm, and iv), an excited-state absorption (ESA) band at ~360 nm. From these pump-probe data alone, the 440 nm band may be interpreted as either an ESA as the system evolves along its excited-state potential energy surface, or a GSA while evolving on the ground-state surface or perhaps even a short-living product-state absorption from a secondary reaction process.

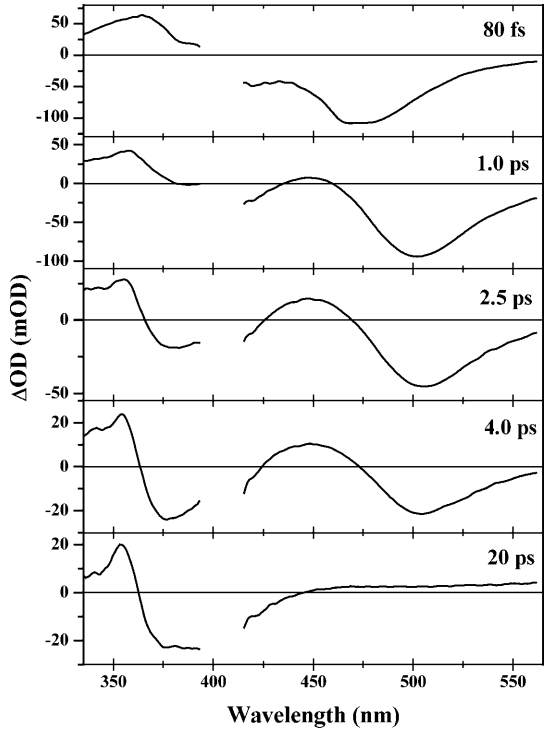

FIGURE 5 Representative dispersion-corrected transient pump-probe spectra of TMpCA. The region around the pump excitation wavelength (400 nm) is corrupted due to scatter from the pump pulse.

Compared to the early time spectra, the 20 ps spectrum shows a markedly different structure. This ''terminal'' TMpCA spectrum exhibits three resolved bands, persists for the duration of the experimental time window (<5 ns), and was initially attributed to the *cis*-isomerized photoproduct (Larsen et al., 2003b). The red-most band in the terminal pump-probe spectrum peaks at ~675 ± 10 nm (peak not shown), which is ascribed to the rather featureless spectrum of hydrated electrons (Freeman and Jou, 1979). This absorbance band is presumably caused by photogenerated hydrated electrons, which suggests that a neutral TMpCA radical absorption band should also be present (and maybe detectable in the probe wavelength range). No clear SE band is observed, which suggests that the excited-state population has completely decayed within 20 ps. Also absent is the absorption band initially observed at 440 nm. The band peaking at 365 nm has shifted to the blue to ~355 nm, is decreased in magnitude, and is distinctly narrower. If the excited-state population is completely relaxed within 20 ps, as is suggested by the lack of an SE band, then the data suggest that the ultraviolet (UV) band contains two bands of different origin, an ESA at early times, that decays quickly, and a ground-state photoproduct band at long times. The relationship between these two bands (i.e., whether they are related sequentially or via parallel paths) is further investigated with the aid of the PDP technique. Between both positive bands is a negative GSB, associated with loss of reacting TMpCA molecules. Because the long time spectrum does not decay within the time range of the experiment, no appreciable recombination kinetics occurs on this timescale.

In contrast to the rapid dynamics observed in TMpCA, the TML chromophore is effectively a dye with a nanosecond excited-state lifetime. Similar spectral features are observed in the pump-probe signals of TML (spectra shown as *solid lines* in Fig. 6, *C* and *D*), including an excited-state absorption in the UV (peaking at 350 nm) and an SE band that is uncluttered with additional ESA. However, in contrast to TMpCA, no positive band at ~440 nm is observed to evolve during the TML photodynamics. As with TMpCA, the SE band does rapidly shift within the first picosecond, which is presumably associated with solvation dynamics (see Discussion). The persistent band that is observed in the terminal spectrum of TMpCA is faintly observed in TML because of its much longer excited-state lifetime.

Pump-dump-probe signals

A powerful aspect of the dispersed PDP spectroscopy technique is that it allows experimentalists to separate and identify overlapping (both spectrally and temporally) bands and to elucidate the underlying connectivity that joins them. With respect to the TMpCA, this entails exploring the dynamics and mechanism behind the transient positive 440 nm band and the nature of the terminal spectrum in the pump-probe data (Fig. 5). The collection and analysis of multiwavelength pump-probe signals has proved useful for understanding the underlying dynamics of the samples studied. However, such dispersed data is equally useful in interpreting single wavelength trace measurements that can be composed of contributions arising from overlapping bands. These benefits gained by collecting dispersed pump-probe signals are also applicable to PDP spectroscopy, and are illustrated in Fig. 6, where three transient spectra (for each

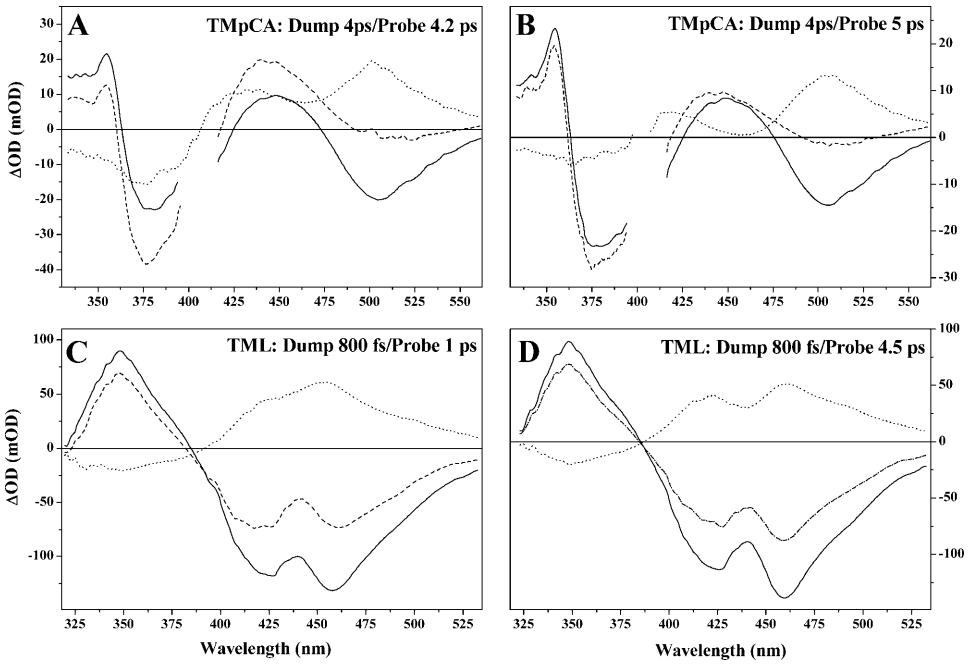

FIGURE 6 Typical dispersed PDP spectra of TMpCA (*A* and *B*) and TML (*C* and *D*). The pump pulse is set at 0 ps; the dump and probe pulse delays are given in each panel. Spectra represent the pump-probe signal (*solid line*), PDP signal (*dashed line*), and the double-difference spectrum, ΔΔOD (*dotted line*), which is calculated from Eq. 1. Note the different wavelength scale for the TMpCA and TML spectra.

specific dump and probe delay time) are presented for typical dispersed PDP experiments on TMpCA and TML. The pump-probe signals of TMpCA (*solid line*) matched those presented in Fig. 5. Overlapping the pump-probe spectra are the PDP signals (*dashed line*), and the double-difference spectrum, ΔΔOD (*dotted line*), which is calculated via Eq. 1.

The ΔΔOD spectra for TMpCA (Fig. 6, *A* and *B*) exhibit i), a decrease in the ESA band at 375 nm, (negative ΔΔOD signal) and ii), a decrease in the SE band at 500 nm (a positive ΔΔOD signal). Both effects are a direct consequence of reducing the excited-state population. In sharp contrast to the positive ESA signals in the UV region, the positive band in the TMpCA spectra at 440 nm does not decrease, but in fact increases upon dumping (positive ΔΔOD signal).

Hence, this positive band at 440 nm is not due to an ESA, but results from a ground-state absorption that is further repopulated through the application of the dump pulse. This ground-state intermediate (GSI) is the result of the dump-induced generation of a nonequilibrated ground-state species absorbing to the red of the equilibrated ground-state spectrum, i.e., absorption spectrum (Fig. 4). After its formation, this GSI decays on a rapid timescale (~1 ps) as it evolves into the equilibrated ground state. The observed GSI may result from several processes, including vibrational cooling, ground-state solvation, or the generation of a structurally perturbed ground-state species, e.g., via twisting of the double bond. Comparing the TMpCA results with TML is used to explore which dynamical contributions are associated with structural rearrangement from the observed GSI relaxation, since the torsional degree of freedom across the double bond is locked by the added ring to the chromophore (Fig. 1).

Similar PDP effects are observed in the TML sample (Fig. 6, *C* and *D*), where the dump pulse induces a loss of ESA (350 nm) and SE (460 nm), while generating a GSI peaking at 445 nm. Key differences between the TML and TMpCA center on the observed relaxation timescales of both the ground- and excited-state dynamics and are further discussed in the following section.

Representative PP and PDP time traces are displayed shown in Fig. 7, highlighting the temporal effects of dumping on the observed transient signals. The pump-probe data for TMpCA exhibits a 2 ps lifetime that has been previously reported (Larsen et al., 2003b), whereas the lifetime of TML stretches over ~3 ns. The PDP data for TMpCA with an early (100 fs; Fig. 7, *blue triangles*) and late (4 ps; *red squares*) dump time display similar properties. The dump-induced loss of excited-state population results in an instrument-limited loss of both the SE (490 nm) and the ESA bands (355 nm). However, the GSI band (440 nm) exhibits an instrument-limited rise and then a rapid ~1 ps decay, which is ascribed to a ground-state relaxation mechanism. As suggested by Fig. 6, the PDP traces measured for TML exhibit similar properties, albeit with differing timescales, compared to TMpCA. After dumping, the GSI traces in TML show an analogous subpicosecond relaxation (Fig. 7, *red*

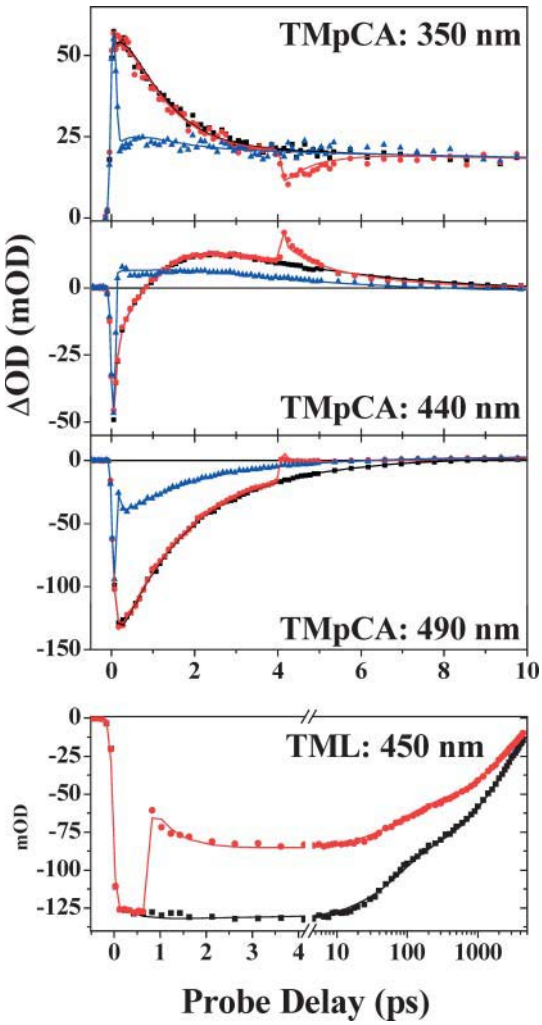

FIGURE 7 Selected pump-probe (*solid squares*) and PDP traces of TMpCA dumped at 100 fs (*solid triangles*) and 4 ps (*solid circles*) and TML dumped at 700 fs (*red circles*). Symbols are the experimental data and the solid lines are the results of the global fits to these data.

circles) that is also ascribed to ground-state relaxation. The comparison between the dynamics of the two systems will be discussed in the context of the global analysis.

The action trace for TMpCA (Fig. 8) collected with the probe time set at 20 ps shows that even though a well-defined pump-probe spectrum is observed (Fig. 5), the presence of the dump pulse at any delay time has no effect on the observed 20 ps transient spectrum. This is observed even though a clear dumping effect is shown in the ''normal'' PDP spectra in Figs. 6 and 7. Hence the dump-induced effect is limited to the induced dynamics on a short timescale after dumping (~2 ps) that is roughly during the excited-state lifetime. The action traces in Fig. 8 show clearly that the species responsible for the 20 ps pump-probe spectrum do not evolve via the excited electronic state, or more specifically, do not evolve through the region of the potential energy surface that can be dumped with the applied dump

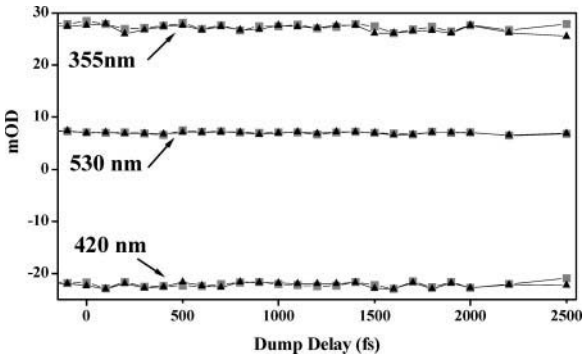

FIGURE 8 Action traces of TMpCA with the probe delay set to 20 ps. The pump-probe traces (*squares*) the 355 nm band, the 420 nm band, and the 550 nm band as a function of the dump delay. PDP traces are shown in triangles.

pulses at 505 nm. If this would have been the case, a change in signal amplitude, due to the population loss via the applied dump pulses, would be observed.

DISCUSSION

Model

Whereas pump-probe signals are particularly sensitive to excited-state dynamics, PDP signals are more sensitive to ground-state dynamics, and the simultaneous fitting of both data sets is required to dissect the observed signals and elucidate the underlying dynamical processes, including both spectral and temporal properties of the constituent species. The connectivity scheme (Eq. 2) used in the global analysis methodology that best describes the data from both TMpCA and TML includes the two processes evolving in parallel: 1), a single-photon excitation evolution, and 2), a multiphoton ionization process (Fig. 9 *A*). We find that the following model fits the data adequately and that there is no need to introduce more complex parameters; also we find that fitting with fewer components gives statistically poorer fits.

The observed dynamics associated with the single-photon excitation includes evolution along both excited and ground electronic potential surfaces and exhibits pronounced spectral changes. The spectral results of the global analysis of the dispersed data are shown in the SADS of Fig. 9, *B* and *C*, and the temporal properties are tabulated in Table 1. Each SADS corresponds to the difference spectrum of a transient state with a specific lifetime; because the SADS is a ''difference spectrum'', it inherently contains a common bleach spectrum and hence exhibits a negative contribution about the absorption spectrum of the sample (Fig. 4). For both TMpCA and TML, three excited-state intermediates (ESI) are observed. TMpCA can be fit with two GSIs, whereas in TML only one is observed. The ESIs spectrally evolve to the red in time until reaching the equilibrated excited-state spectrum (if possible) and the GSIs evolve to

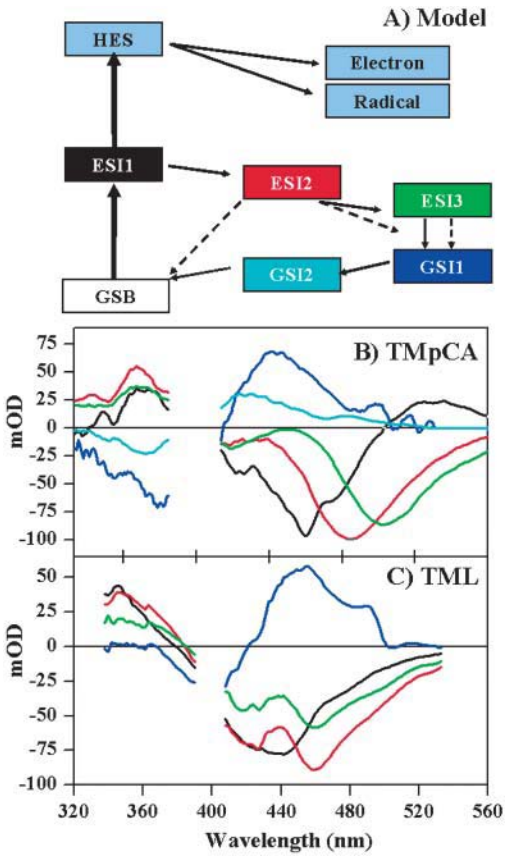

FIGURE 9 Global analysis results derived from the PDP and pump-probe data: (*A*) Connectivity scheme used in the modeling of the pump-probe and PDP data. ESI1, ESI2, and ESI3 refer to the excited-state intermediates No. 1, No. 2, and No. 3, respectively. GSB is the equilibrated ground-state species, and GSI1 and GSI2 are ground-state intermediates. Solid arrows represent the pump-probe population dynamics, and the dashed arrows represent the population dynamics induced by dumping at early times (from ESI2) or at late times (from ESI3). HES is a higher lying excited electronic state that leads directly to ionization. (*B*) Species associated difference spectra (SADS) of each transient state of TMpCA. (*C*) SADS extracted for TML with the same connectivity scheme, but with only one GSI. The spectra are color-coded to the colors of the transient states in *A*. Not shown is the spectrum associated with the neutral radical, solvated electron, and partial bleach spectrum, which is identical to the 20 ps spectrum in Fig. 5 for TMpCA.

the blue until reaching the equilibrated ground-state absorption. The dynamics of these evolutions are of interest when investigating isomerization dynamics.

For TMpCA, the SADS of each ESI exhibits a strong SE band that peaks between 460 nm and 510 nm and an ESA in the near-UV region that does not shift appreciably with time. The SE of the first excited-state intermediate, ESI1 (Fig. 9, *black curve*), peaks at ~460 nm and shifts to 480 nm to form ESI2 (*red curve*) within 100 fs. An additional red shift occurs, as ESI2 shifts to the third excited-state intermediate, ESI3 (*green curve*), on a 500 fs timescale. The 2 ps decay of the ESI3 state is a purely kinetic process and exhibits no spectral shifting. These extracted SADS are in near-

TABLE 1 Transient state lifetimes

	Excited-state species			Ground-state species		
State	ESI1	ESI2	ESI3	GSI1	GSI2	Rad/e$^-$
TMpCA	75 ± 20 fs	470 ± 50 fs	2.1 ± 0.2 ps	240 ± 100 fs	1.4 ± 0.1ps	∞
TML	400 ± 50 fs	73 ± 2 ps	2.2 ± 0.1 ns	500 ± 50 fs	-	∞

Exponential lifetimes of the transient states estimated from the simultaneous global analysis of the measured pump-probe and PDP data.

quantitative agreement with unpublished time-resolved fluorescence measurements.

Similar dynamics are observed in TML; however, the spectral evolution is confined to the ESI1 → ESI2 transition on a 400 fs timescale, whereas both ESI2 and ESI3 exhibit purely kinetic decays, with time constants of 73 ps and 2.2 ns, respectively. In contrast to the 50-nm shift that the ESIs of TMpCA evolve through, the spectral shift of the ESIs in TML is ~10 nm (440 nm for ESI1 and 450 nm for ESI2 and ESI3). This indicates that the degree of excited-state relaxation occurring in TML is much less than in TMpCA.

After excitation of either chromophore, the system (both the chromophore and the aqueous solvent environment) finds itself in a nonequilibrated state and will be subject to the forces associated with the excited-state potential surface, with a different charge distribution. The system will subsequently relax along a multidimensional excited-state potential energy surface that dictates the evolution of the system. Characterizing this potential energy surface is key to unlocking the dynamics of the chromophore and is a central goal in these measurements. The excited-state relaxation includes contributions from both intramolecular motions (e.g., bond lengthening) and more specifically torsion (e.g., around the double bond dihedral angle), and intermolecular motions, such as solvent rotations and translations that are commonly grouped together within the field of solvation dynamics. The separation of the observed red-shifting dynamics into these different origins is difficult. Moreover, the solvent dynamics and the chromophore dynamics are coupled, leading to further complexity in the interpretation. The comparison of data from TMpCA and TML is a first step in dissecting the potential energy surface for the PYP chromophore.

The 100-fs and 500-fs timescales of the first two ESIs of TMpCA are comparable with previous measurements of aqueous solvation (Jimenez et al., 1994; Jordanides et al., 1999) and are ascribed to intermolecular solvent motions (i.e., excited-state solvation dynamics). Since the excited-state lifetime of TMpCA is strongly quenched (2 ps lifetime), it is likely that the rapid internal conversion originates from the torsion about the double bond dihedral angle.

The 400-fs red shift in the ESIs of TML is also ascribed to solvation dynamics due to the similarities to TMpCA. The locking of the central double bond in TML extends the excited-state lifetime out to nanoseconds, presumably because the internal conversion pathway induced by twisting is blocked. The TML excited state exhibits a biexponential decay curve (Fig. 7) that may result either from inhomogeneity of the ground state or inherent nonexponential dynamics of the excited state. Since TML is a rigid molecule (Fig. 1) with only one degree of freedom (rotation about the single bond toward the carbonyl atom), this would be the only source of inhomogeneity. However, steric factors from the bulky thio-methyl group would make the ground-state inhomogeneity argument unlikely. The other option is more plausible: it may be possible that when TML is in its excited state, rotation about this single bond in the TML molecule can be more flexible and this rotamer may lead to enhanced internal conversion. Ab initio calculations would be able to address this issue and highlight the role of excited-state relaxation due to motions of other bonds.

After dumping of the excited chromophores to the ground-state potential surface, the system will start to relax on the ground electronic surface. The two ground-state intermediates observed in the global fits for TMpCA (Fig. 9 *A*, *blue* and *cyan curves*) result from the ground-state counterpart to excited-state dynamics, and as with the ESIs, the GSIs exhibit distinct spectral evolution. The first ground-state intermediate in TMpCA, GSI1 (*blue curve*), peaks at 440 nm and rapidly relaxes to GSI2 (*cyan curve*) within 200 fs. Then GSI2 relaxes fully into the GSB on a 1.4-ps timescale. Both ground-state relaxation steps encompass ~30 nm in blue shift. In contrast to the biexponential relaxation observed in TMpCA, the single-exponential ground-state relaxation of TML evolves faster (500 fs).

Three processes potentially contribute to the observation of the GSIs in these PDP experiments: 1), vibrational cooling of ''hot'' molecules, 2), ground-state solvation, and 3), the reversal of structural motion occurring in the excited state (e.g., torsion about a dihedral angle of TMpCA). Whereas all three processes are potential candidates for ground-state relaxation in TMpCA, in TML the last option is excluded by the locking ring. The linear response approximation postulates that ground-state solvation occurs on comparable timescales as excited-state solvation and has been shown to hold in several ground-state solvation dynamics studies (Changenet-Barret et al., 2000; Kovalenko et al., 1998). The similarity of the ground-state (500 fs) and excited-state (400 fs) dynamics of TML supports the claim that solvation dynamics contributes significantly to the ground-state dynamics.

Vibrational cooling results from the thermalization of the ''hot'' ground electronic state after the rapid introduction of excess vibrational energy. In the PDP probe experiments, the

maximum amount of energy that can be introduced into the ground state would be the energy difference between the pump pulse (25,000 cm^{-1}) and the dump pulse (19,800 cm^{-1}). However, this estimate does not include the dissipation of energy in the excited state due to solvation and vibrational cooling before dumping. In viscosity-dependent pump-probe measurements (presented elsewhere), the timescales of both the ground-state and excited-state relaxation dynamics are strongly correlated with viscosity. This is a dependence expected for the slower aspects of solvation dynamics, which depend on macroscopic collective motions of the solvent (Horng et al., 1995), but not necessarily expected for vibrational cooling of large molecules.

Despite this support for ascribing the ground-state solvation process as the explanation for the observed relaxation of GSI, it does not explain the results of PDP experiments on the PYP protein (D. S. Larsen, I. H. M. van Stokkum, M. Vengris, M. van der Horst, K. Hellingwerf, and R. van Grondelle, unpublished), where a GSI is observed with a lifetime of ~4 ps. Since this timescale is much slower than previous studies of protein solvation (Changenet-Barret et al., 2000), we turn to the third hypothesis for the observed ground-state relaxation.

The freedom of rotation about the central double bond of TMpCA is responsible for the fast internal conversion, and after hopping to the ground state, the molecule must find itself in a nonequilibrated, twisted conformation. This twisted state must return back to its original conformation subject to the nature of the ground-state potential energy surface. We postulate that the ground-state dynamics are sensitive to this readjustment of the double bond back to the original *trans* configuration. The faster rate of ground-state torsion (1.4 ps) versus excited-state torsion (2.1 ps) is indicative of a deeper potential well for isomerization in the ground electronic state than in the excited electronic state (Ben-Amotz and Harris, 1987a,b), which is expected for the $\pi \rightarrow \pi^*$ transition predicted for the PYP molecule (Molina and Merchan, 2001).

The observation of these timescales provides a kinetic understanding of the dynamics occurring within TMpCA, but not necessarily a microscopic understanding. The ultimate goal of these multipulse studies is to extract the information that is required to construct the potential energy surfaces that describe the photoinduced structural dynamics, and from this understand how proteins interact and tune these potential energy surfaces to result in a desired biological function (e.g., initiation of the PYP photocycle). To accomplish this, an isomerization model must be adopted and compared with our results that is either based on a phenomenological (Bagchi et al., 1983; Oster and Nishijima, 1956) or ab initio (Garavelli et al., 2003; Quenneville and Martínez, 2003) approach. Recently, Martínez and co-workers (Ko et al., 2003) have directed their ab initio techniques to explore the dynamics of neutral pCA in the gas phase to explore the energetics of internal conversion from the excited-state potential energy surface. It is clear that to support a reliable model for the TMpCA photoreaction, its dependence on different conditions (e.g., different solvents, temperature, viscosity and chemical composition, and excitation wavelength) must be explored; results of such studies will be presented elsewhere.

The separation of the multiple pathway dynamics in TMpCA highlights a powerful aspect of PDP spectroscopy that is useful for studying complicated dynamical systems. In both chemical and biological systems, complex connectivity schemes that model the underlying relationship (e.g., excitation energy flow, electronic-state hopping, and structural intermediates) between different transient states are quite common (Gobets et al., 2001; Holzwarth, 1996; Krueger et al., 2002; Papagiannakis et al., 2002). Despite the ability to identify spectral and temporal properties in wavelength- and time-resolved pump-probe measurements, the connectivity between the observed spectral states may be difficult to identify unambiguously with such measurements. The introduction of an additional de-excitation pulse in PDP spectroscopy provides direct experimental information to separate signals originating from ground- and excited-state intermediates.

Power dependence

The power dependence of the terminal spectrum of TMpCA was investigated to further identify the nature of the species that constitute the terminal spectrum and the mechanism(s) that generate them. The PDP action trace (Fig. 8) shows that the terminal spectrum exhibits no dependence on the dump time and thus the species constituting these bands consequentially evolve in parallel with the observed quenching photodynamics. More specifically, since the 505-nm dump wavelength is poorly resonant with ESI1, any dumping of this state would be poorly observed.

Assuming that any isomerized photoproducts generated would evolve via the excited electronic state, the action traces imply that no persistent photoisomerization products are formed for TMpCA in solution. This is an interesting result because of the inclination of pCA (lacking a thiomethyl linkage) to photoisomerize both in solution (Aulin-Erdtman and Sanden, 1968; Changenet-Barret et al., 2001) and in the gas phase (Ryan et al., 2002). In addition, many experimental studies show a clear isomerization of the chromophore in the PYP protein environment (Genick et al., 1997, 1998; Perman et al., 1998). Therefore, the addition of the thiomethyl linkage to the *p*-coumaric acid chromophore (present in both TMpCA and PYP) changes the photodynamics of the bare chromophore (Changenet-Barret et al., 2002). Thus, the protein environment plays an important and vital role in activating and facilitating the configurational transition of the chromophore in PYP.

Fig. 10 *A* shows the power dependence of the 20 ps pump-probe spectrum for TMpCA. As the pulse energy is varied

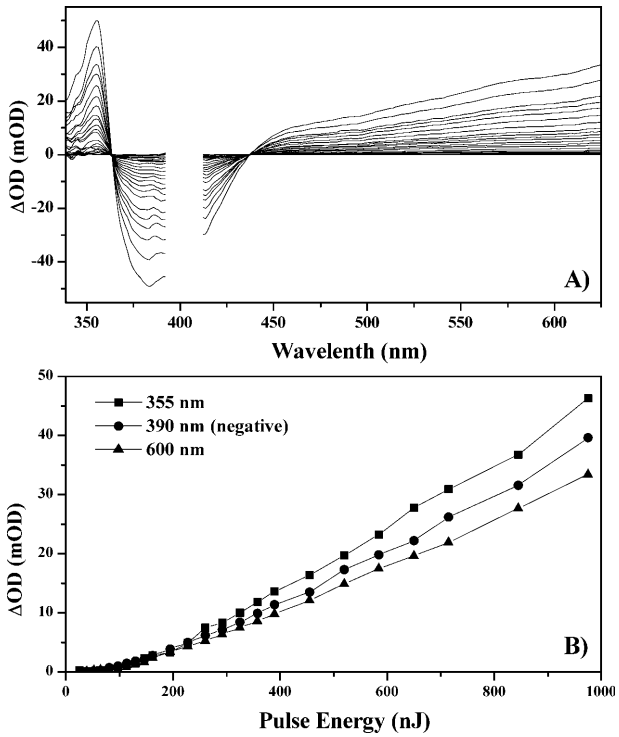

FIGURE 10 Power-dependent change in the dispersed pump-probe signals of the terminal spectrum of TMpCA. Pulse energy was varied from 15 nJ/pulse to 1 μJ/pulse. (*A*) Power dependence of the 20-ps pump-probe spectrum. (*B*) Power dependence of the three distinct bands. The values of the radical band (*solid squares*), bleach band (*solid circles*), and electron band (*solid triangles*) were measured at 350 nm, 390 nm, and 600 nm, respectively. The negative signal of the bleach band was plotted to help in comparison to the other bands.

from 10 nJ/pulse to 500 nJ/pulse, the magnitude of all three bands follows the same intensity dependence, which is further corroborated by the observation of two isosbestic points, at ~365 nm and 475 nm. Hence, the species that give rise to these bands follow the same power dependence and presumably arise from the same mechanism.

The red-most band peaks at ~675 nm (not shown), which agrees with the experimentally observed spectrum of solvated electrons (Freeman and Jou, 1979). The negative band at 380 nm resembles the ground-state bleach and the band that peaks at 355 nm may be attributed to the neutral TMpCA radical resulting from ionization, instead of a persistent isomerization photoproduct (Changenet-Barret et al., 2001). Since this UV band follows the same power dependence as the band caused by the hydrated electron (and the corresponding bleach) and closely resembles the radical spectrum measured for the *p*-coumaric acid analogue (Foley et al., 1999), it is more likely that the UV band originates from the radical spectrum and not from a photogenerated isomer.

The power dependence of these three bands is shown in Fig. 10 *B* and exhibits a pseudo-linear trend. At lower pulse energies, a weak quadratic dependence is observed, whereas at higher energies, the power dependence turns linear. A linear trend was expected for a single photon mechanism, as expected for the TMpCA isomerization process, and thus this radical band was previously suggested to be the *cis* photoisomer (Larsen et al., 2003b). A single-photon electron detachment mechanism was not expected to occur with the low energy photons in the 400-nm excitation pulse, and a pure two-photon transition is expected to exhibit a quadratic power dependence. The observed pseudo-linear power dependence can, however, be explained as a result of a resonantly enhanced two-photon transition that proceeds via the first excited electronic state (more specifically ESI1).

We can describe the power dependence with the kinetic scheme in the inset of Fig. 11. In this model, four states are linearly coupled, whereas to ionize the TMpCA chromophore, two high-energy photons are required: 1), one resonant with the ground-state absorption, and 2), one resonant with the excited-state absorption. After double excitation, the 50,000 cm^{-1} of excess energy is enough to overcome the ionization threshold and detach the electron into the solvent. The dynamics of the population of the different states (including the formation of radicals) can then be described by the following system of nonlinear differential equations (Gai et al., 1997; Logunov et al., 2001):

$$\frac{dn_0}{dt} = -\boldsymbol{k}_{01S}I(t)n_0 + \boldsymbol{k}_{10S}I(t)n_1 + \boldsymbol{k}_{10}n_1 \tag{4a}$$

$$\frac{dn_1}{dt} = \boldsymbol{k}_{01S}I(t)n_0 - \boldsymbol{k}_{10S}I(t)n_1 - \boldsymbol{k}_{12S}I(t)n_1 + \boldsymbol{k}_{21S}I(t)n_2 - \boldsymbol{k}_{10}n_1 + \boldsymbol{k}_{21}n_2 \tag{4b}$$

$$\frac{dn_2}{dt} = \boldsymbol{k}_{12S}I(t)n_1 - \boldsymbol{k}_{21S}I(t)n_2 - \boldsymbol{k}_{21}n_2 - \boldsymbol{k}_{23}n_2 \tag{4c}$$

$$\frac{dn_3}{dt} = \boldsymbol{k}_{23}n_2, \tag{4d}$$

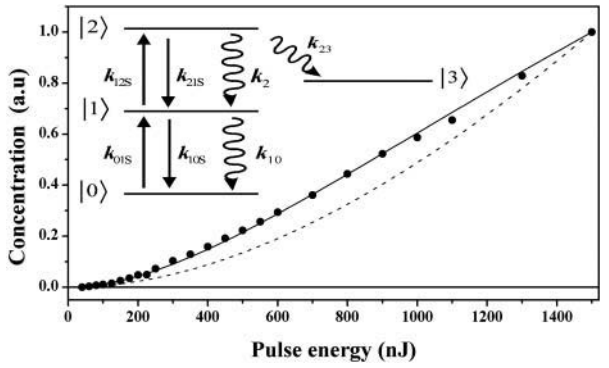

FIGURE 11 Comparison of four-state model results with experimental electron band power dependence. Measured (*solid circles*) and modeled (*solid line*) power dependence of radical/electron formation. The dashed line shows the modeled power dependence for the hypothetical case, were S_1 would relax very fast. Inset shows the applied four-state kinetic model.

where n_i ($i = 0,1,2$) are the fractional population of the S_0, S_1, and S_2 electronic states, respectively; n_3 is the solvated electron and radical concentration. The electronic states are coupled via either external electric fields (e.g., originating from a photon) with extinction coefficients for absorption and stimulated emission transitions, $\boldsymbol{k}_{ijS}$, from the ith to jth electronic state, or via spontaneous relaxation (and internal conversion) pathways where $\boldsymbol{k}_{21}$ and $\boldsymbol{k}_{10}$ are the natural decay times of the S_2 and S_1 states, respectively. The rate of radical formation from S_2 is $\boldsymbol{k}_{23}$ and the Gaussian intensity profile (number of photons) of the excitation pulse is $I(t)$.

The above differential equations were solved numerically with a Runge-Kutta algorithm (MATLAB, The MathWorks, Natick, MA). The calculated power dependence from these equations, with the parameters in Table 2, satisfactorily describes the observed power dependence of the radical/electron formation (Fig. 11). Since the excited-state absorption dominates the ground-state bleach (Figs. 5 and 6) around the excitation wavelength, its extinction coefficient $\boldsymbol{k}_{12S}$ is thus greater than that of the ground-state absorption $\boldsymbol{k}_{01S}$.

The pseudo-linear two-photon power dependence of the radical formation originates from two factors in the model: 1), the $S_2 \leftarrow S_1$ transition is more strongly coupled to the excitation pulse than the $S_1 \leftarrow S_0$ transition, and 2), the S_1 state lifetime is longer than the excitation pulse width. This combination of factors leads to a saturation of the S_1 electronic state population at high pulse intensities. At lower pulse intensities, the power dependence behaves more like the quadratic dependence expected for a two-photon transition because of the small population in the S_1 electronic state. The dashed curve in Fig. 11 illustrates that that when the lifetime of the S_1 state is set to a short value ($\boldsymbol{k}_{10} = 1$ fs^{-1}), where no accumulation of an excited-state population occurs in S_1, the predicted power dependence is more curved in accordance with a true two-photon transition.

Since the radical is formed via a two-photon transition that is resonantly enhanced with two sequential single-photon transitions, both with an appreciable extinction coefficient (Table 2), this pathway cannot be prevented by decreasing the excitation power without also increasing the relative noise level of the single-photon signals to an unacceptable level. An alternative and more useful way to suppress the ionization pathway would be to excite the system at a wavelength that has good overlap with the ground-state absorption and poor overlap with the excited-state absorption. However, a comparison of these two bands (Figs. 4 and 9) shows that such an ideal wavelength does not exist for this chromophore (at least not >330 nm).

TABLE 2 Initial excitation parameters

Parameter	Value	Units
$\boldsymbol{k}_{01S}$, $\boldsymbol{k}_{10S}$	45,000	cm^2/mmol
$\boldsymbol{k}_{12S}$, $\boldsymbol{k}_{21S}$	112,500	
$\boldsymbol{k}_{10}$	1/1800	fs^{-1}
$\boldsymbol{k}_{21}$, $\boldsymbol{k}_{23}$	1/30	

The parameters used to describe the power dependence of radical formation in TMpCA with the model shown in the inset of Fig. 11 and the differential equations of Eq. 4. The ground-state absorption extinction coefficient was taken from Kroon et al. (1996).

CONCLUDING REMARKS

We collected both dispersed pump-probe and pump-dump-probe signals on the TMpCA chromophore in solution, as a model system for studying the dynamics of the PYP chromophore, without the effects of the protein environment. The collected frequency- and time-resolved data were analyzed with a global analysis program that models both the pump-probe and the PDP data simultaneously within a single connectivity scheme. From the pump-probe results alone, information concerning the excited-state dynamics can be extracted that highlights several distinct excited-state intermediates that are attributed to both solvation dynamics and intramolecular structural rearrangement (e.g., torsion around (the double) bond(s) of the chromophore) and ultrafast quenching of the excited state. In combination with the PDP signals, detailed information about the resulting ground-state intermediates can be extracted, which provides direct feedback on the nature of the ground electronic state potential energy surface; this can be especially useful for the characterization of these potentials in future theoretical studies (Abramavicius et al., 2002).

The connectivity scheme that best models the data includes two parallel processes involving i), a single-photon absorption dynamics pathway, and ii), a resonantly enhanced two-photon ionization process. Our PDP investigation shows that even though the excited electronic state for the TMpCA chromophore in solution is quenched, no persistent isomerized photoproduct is observed (only ionization products are observed on long timescales (10 ps)). This is in contrast to results obtained with the same chromophore when it is covalently bound to the PYP protein, where the isomerization process triggers a photocycle (with a quantum yield of 0.35) (van Brederode et al., 1995; Cusanovich and Meyer, 2003; Hellingwerf et al., 2003) that eventually results in a phototaxis response in the bacterium. The comparison of these two systems highlights the complex and important role that proteins have in tuning intraprotein reactions into productive biological function.

The TMpCA system is a useful system to explore the PYP dynamics, since the obscuring effects of the photocycle do not interfere with the observed TMpCA photodynamics. The two major observations in this study are the observation of a ground-state relaxation explained as a result of failed isomerization (partial torsion) attempts and the identification and characterization of a resonantly enhanced ionization pathway that generated detached electrons and radicals. Additional PDP data collected on PYP protein samples exhibit both resolvable ground-state dynamics and the photodetachment reaction products, and will be discussed elsewhere.

D.S.L. is grateful to the Human Frontier Science Program Organization for providing financial support with a long-term fellowship.

This research was supported by the Netherlands Organization for Scientific Research via the Dutch Foundation for Earth and Life Sciences.

REFERENCES

Abramavicius, D., V. Gulbinas, L. Valkunas, Y.-J. Shiu, K. Liang, M. Hayashi, and S. Lin. 2002. Molecular twisting and relaxation in the excited state of triarylpyrylium cations. *J. Phys. Chem. A.* 106:8864–8869.

Aulin-Erdtman, G., and R. Sanden. 1968. Spectrographic contributions to lignin chemistry. *Acta Chem. Scan.* 22:1187–1209.

Baca, M., G. E. Borgstahl, M. Boissinot, P. M. Burke, D. R. Williams, K. A. Slater, and E. D. Getzoff. 1994. Complete chemical structure of photoactive yellow protein: novel thioester-linked 4-hydroxycinnamyl chromophore and photocycle chemistry. *Biochemistry.* 33:14369–14377.

Bagchi, B., G. R. Fleming, and D. W. Oxtoby. 1983. Theory of electronic relaxation in solution in the absence of an activation barrier. *J. Chem. Phys.* 78:7375–7385.

Baltuška, A., I. H. M. van Stokkum, A. Kroon, R. Monshouwer, K. J. Hellingwerf, and R. van Grondelle. 1997. The primary events in the photoactivation of yellow protein. *Chem. Phys. Lett.* 270:263–266.

Ben-Amotz, D., and C. Harris. 1987a. Torsional dynamics of molecules on barrierless potentials in liquids. 1. Temperature and wavelength dependent picosecond studies of triphenylmethane dyes. *J. Chem. Phys.* 86:4856–4870.

Ben-Amotz, D., and C. Harris. 1987b. Torsional dynamics of molecules on barrierless potentials in liquids. 2. Test of theoretical models. *J. Chem. Phys.* 86:5433–5440.

Brudler, R., R. Rammelsberg, T. T. Woo, E. D. Getzoff, and K. Gerwert. 2001. Structure of the I1 early intermediate of photoactive yellow protein by FTIR spectroscopy. *Nat. Struct. Biol.* 8:265–270.

Changenet-Barret, P., C. Choma, E. Gooding, W. DeGrado, and R. M. Hochstrasser. 2000. Ultrafast dielectric response of proteins from dynamics stokes shifting of coumarin in calmodulin. *J. Phys. Chem. B.* 104:9322–9329.

Changenet-Barret, P., A. Espagne, N. Katsonis, S. Charier, J.-B. Baudin, L. Jullien, P. Plaza, and M. M. Martin. 2002. Excited-state relaxation dynamics of a PYP chromophore model in solution: influence of the thioester group. *Chem. Phys. Lett.* 365:285–291.

Changenet-Barret, P., P. Plaza, and M. M. Martin. 2001. Primary events in the photoactive yellow protein chromophore in solution. *Chem. Phys. Lett.* 336:439–444.

Cusanovich, M. A., and T. E. Meyer. 2003. Photoactive yellow protein: a prototypic PAS domain sensory protein and development of a common signaling mechanism. *Biochemistry.* 42:4759–4770.

Chosrowjan, H., N. Mataga, Y. Shibata, Y. Imamoto, and F. Tokunaga. 1998. Environmental effects on the femtosecond-picosecond fluorescence dynamics of photoactive yellow protein: chromophores in aqueous solutions and in protein nanospaces modified by site-directed mutagenesis. *J. Phys. Chem. B.* 102:7695–7698.

Foley, S., S. Navaratnam, D. J. McGarvey, E. J. Land, T. G. Truscott, and C. A. Rice-Evans. 1999. Singlet oxygen quenching and the redox properties of hydroxycinnamic acids. *Free Radic. Biol. Med.* 26:1202–1208.

Freeman, G. R., and F.-Y. Jou. 1979. Temperature and isotope effects on the shape of the optical absorption spectrum of solvated electrons in water. *J. Phys. Chem.* 83:2383–2387.

Gai, F., J. C. McDonald, and P. Anfinrud. 1997. Pump-dump-probe spectroscopy of bacteriorhodopsin: evidence for a near-IR excited state absorbance. *J. Am. Chem. Soc.* 119:6201–6202.

Garavelli, M., F. Ruggeri, F. Ogliaro, M. J. Bearpark, F. Bernardi, M. Olivucci, and M. A. Robb. 2003. A simple approach for improving the hybrid MMVB force field: application to the photoisomerization of s-cis butadiene. *J. Comput. Chem.* 24:1357–1363.

Genick, U. K., G. E. Borgstahl, K. Ng, Z. Ren, C. Pradervand, P. M. Burke, V. Srajer, T. Y. Teng, W. Schildkamp, D. E. McRee, K. Moffat, and E. D. Getzoff. 1997. Structure of a protein photocycle intermediate by millisecond time-resolved crystallography. *Science.* 275:1471–1475.

Genick, U. K., S. M. Soltis, P. Kuhn, I. L. Canestrelli, and E. D. Getzoff. 1998. Structure at 0.85 Å resolution of an early protein photocycle intermediate. *Nature.* 392:206–209.

Gensch, T., C. C. Gradinaru, I. H. M. van Stokkum, J. Hendriks, K. Hellingwerf, and R. van Grondelle. 2002. The primary photoreaction of photoactive yellow protein (PYP): anisotropy changes and excitation wavelength dependence. *Chem. Phys. Lett.* 356:347–354.

Gobets, B., J. T. M. Kennis, J. A. Ihalainen, M. Brazzoli, R. Croce, I. H. M. van Stokkum, R. Bassi, J. P. Dekker, H. van Amerongen, G. R. Fleming, and R. van Grondelle. 2001. Excitation energy transfer in dimeric light harvesting complex I: a combined streak-camera/fluorescence upconversion study. *J. Phys. Chem. B.* 105:10132–10139.

Gradinaru, C. C., I. H. M. van Stokkum, A. A. Pascal, R. van Grondelle, and H. van Amerongen. 2000. Identifying the pathways of energy transfer between carotenoids and chlorophylls in LHCII and CP29. A multicolor pump-probe study. *J. Phys. Chem. B.* 104:9330–9342.

Hellingwerf, K. J., J. Hendriks, and T. Gensch. 2003. Photoactive yellow protein, a new type of photoreceptor protein: Will this ''yellow lab'' bring us where we want to go? *J. Phys. Chem. A.* 107:1082–1094.

Hoff, W. D., P. Dux, K. Hard, B. Devreese, I. M. Nugteren-Roodzant, W. Crielaard, R. Boelens, R. Kaptein, J. van Beeumen, and K. J. Hellingwerf. 1994a. Thiol ester-linked p-coumaric acid as a new photoactive prosthetic group in a protein with rhodopsin-like photochemistry. *Biochemistry.* 33:13959–13962.

Hoff, W. D., I. H. M. van Stokkum, H. J. van Ramesdonk, M. E. van Brederode, A. M. Brouwer, J. C. Fitch, T. E. Meyer, R. van Grondelle, and K. J. Hellingwerf. 1994b. Measurement and global analysis of the absorbance changes in the photocycle of the photoactive yellow protein from *Ectothiorhodospira halophila*. *Biophys. J.* 67:1691–1705.

Holzwarth, A. R. 1996. Data analysis in time-resolved measurements. *In* Biophysical Techniques in Photosynthesis. J. Amesz and A. J. Hoff, editors. Kluwer, Dordrecht, The Netherlands.

Horng, M. L., J. A. Gardecki, A. Papazyan, and M. Maroncelli. 1995. Subpicosecond measurements of polar solvation dynamics—coumarin 153 revisited. *J. Phys. Chem.* 99:17311–17337.

Ishikawa, H., C. Nagao, N. Mikami, and R. Field. 1997. Observation of the ''isomerization states'' of HCP by stimulated emission pumping spectroscopy: comparison between theory and experiment. *J. Chem. Phys.* 106:2980–2983.

Jimenez, R., G. R. Fleming, P. V. Kumar, and M. Maroncelli. 1994. Femtosecond solvation dynamics of water. *Nature.* 369:471–473.

Jordanides, X. J., M. J. Lang, X. Y. Song, and G. R. Fleming. 1999. Solvation dynamics in protein environments studied by photon echo spectroscopy. *J. Phys. Chem. B.* 103:7995–8005.

Ko, C., B. Levine, A. Toniolo, L. Monohar, S. Olsen, H.-J. Werner, and T. J. Martinez. 2003. Ab initio excited-state dynamics of the photoactive yellow protein chromophore. *J. Am. Chem. Soc.* 125:12710–12711.

Kort, R., H. Vonk, X. Xu, W. D. Hoff, W. Crielaard, and K. J. Hellingwerf. 1996. Evidence for trans-cis isomerization of the p-coumaric acid chromophore as the photochemical basis of the photocycle of photoactive yellow protein. *FEBS Lett.* 382:73–78.

Kovalenko, S. A., J. Ruthmann, and N. P. Ernsting. 1998. Femtosecond hole-burning spectroscopy with stimulated emission pumping and supercontinuum probing. *J. Chem. Phys.* 109:1894–1900.

Kroon, A. R., W. D. Hoff, H. P. Fennema, J. Gijzen, G. J. Koomen, J. W. Verhoeven, W. Crielaard, and K. J. Hellingwerf. 1996. Spectral tuning, fluorescence, and photoactivity in hybrids of photoactive yellow protein, reconstituted with native or modified chromophores. *J. Biol. Chem.* 271:31949–31956.

Krueger, B. P., S. S. Lampoura, I. H. M. van Stokkum, E. Papagiannakis, J. M. Salverda, C. C. Gradinaru, D. Rutkauskas, R. G. Hiller, and R. van

Grondelle. 2002. Energy transfer in the peridinin chlorophyll-a protein of *Amphidinium carterae* studied by polarized transient absorption and target analysis. *Biophys. J.* 80:2843–2855.

Larsen, D. S., E. Papagiannakis, I. H. M. van Stokkum, M. Vengris, J. T. M. Kennis, and R. van Grondelle. 2003a. Excited state dynamics of β-carotene explored with dispersed multi-pulse experiments. *Chem. Phys. Lett.* 381:733–742.

Larsen, D. S., M. Vengris, I. H. M. van Stokkum, M. van der Horst, R. Cordfunke, K. J. Hellingwerf, and R. van Grondelle. 2003b. Initial photo-induced dynamics of the photoactive yellow protein chromophore in solution. *Chem. Phys. Lett.* 369:563–569.

Logunov, S. L., V. V. Volkov, M. Braun, and M. A. El-Sayed. 2001. The relaxation dynamics of the excited electronic states of retinal in bacteriorhodopsin by two-pump probe femtosecond studies. *Proc. Natl. Acad. Sci. USA.* 98:8475–8479.

Molina, V., and M. Merchan. 2001. On the absorbance changes in the photocycle of the photoactive yellow protein: a quantum-chemical analysis. *Proc. Natl. Acad. Sci. USA.* 98:4299–4304.

Oster, G., and Y. Nishijima. 1956. Fluorescence and internal rotation: their dependence on viscosity of the medium. *J. Am. Chem. Soc.* 78:1581–1584.

Papagiannakis, E., J. T. M. Kennis, I. H. M. van Stokkum, R. J. Cogdell, and R. van Grondelle. 2002. An alternative carotenoid-to-bacteriochlorophyll energy transfer pathway in photosynthetic light harvesting. *Proc. Natl. Acad. Sci. USA.* 99:6017–6022.

Perman, B., V. Srajer, Z. Ren, T. Teng, C. Pradervand, T. Ursby, D. Bourgeois, F. Schotte, M. Wulff, R. Kort, K. Hellingwerf, and K. Moffat. 1998. Energy transduction on the nanosecond time scale: early structural events in a xanthopsin photocycle. *Science.* 279:1946–1950.

Pique, J., Y. Engel, R. Levine, Y. Chen, R. Field, and J. Kinsery. 1988. Broad spectral features in the stimulated-emission pumping of acetylene. *J. Chem. Phys.* 88:5972–5974.

Quenneville, J., and T. J. Martínez. 2003. Ab initio study of cis-trans photoisomerization in stilbene and ethylene. *J. Phys. Chem. A.* 107:829–837.

Rice, S. A., and M. Zhao. 2000. Optical Control of Molecular Dynamics. Wiley Interscience, New York.

Ruhman, S., B. Hou, N. Freidman, M. Ottolenghi, and M. Sheves. 2002. Following evolution of bacteriorhodopsin in its reactive excited state via stimulated emission pumping. *J. Am. Chem. Soc.* 124:8854–8858.

Ryan, W., D. J. Gordon, and D. H. Levy. 2002. Gas phase photochemistry of the photoactive yellow protein chromophore trans-p-coumaric acid. *J. Am. Chem. Soc.* 124:6194–6201.

Sprenger, W. W., W. D. Hoff, J. P. Armitage, and K. J. Hellingwerf. 1993. The eubacterium *Ectothiorhodospira halophila* is negatively phototactic, with a wavelength dependence that fits the absorption spectrum of the photoactive yellow protein. *J. Bacteriol.* 175:3096–3104.

van Brederode, M. E., T. Gensch, W. D. Hoff, K. J. Hellingwerf, and S. E. Braslavsky. 1995. Photoinduced volume change and energy storage associated with the early transformations of the photoactive yellow protein from *Ectothiorhodospira halophila*. *Biophys. J.* 63:1101–1109.

Xie, A., W. D. Hoff, A. R. Kroon, and K. J. Hellingwerf. 1996. Glu46 donates a proton to the 4-hydroxycinnamate anion chromophore during the photocycle of photoactive yellow protein. *Biochemistry.* 35:14671–14678.

Xie, A., L. Kelemen, J. Hendriks, B. J. White, K. J. Hellingwerf, and W. D. Hoff. 2001. Formation of a new buried charge drives a large-amplitude protein quake in photoreceptor activation. *Biochemistry.* 40:1510–1517.

Yan, M., L. Rothberg, and R. Callender. 2001. Femtosecond dynamics of rhodopsin photochemistry probed by double pump spectroscopic approach. *J. Phys. Chem. B.* 105:856–859.

Zhou, Y., L. Ujj, T. E. Meyer, M. A. Cusanovich, and G. H. Atkinson. 2001. Photocycle dynamics and vibrational spectroscopy of the E46Q mutant of photoactive yellow protein. J. Phys. Chem. A. 105:5719–5726.